INTERPLANETARY ENERGETIC PARTICLES, CORONAL FLARES, AND HARD X-RAY MICROFLARES

(Invited)

Robert P. Lin

Space Sciences Laboratory, University of California, Berkeley, CA 94720 U.S.A.

ABSTRACT

We review solar electron phenomena which can produce low levels of hard X-ray emission at the Sun. Small ~2 to 100 keV solar electrons events, the most common type of impulsive solar particle emission, appear to originate in flare-like bursts high in the corona. These events often are accompanied by ~1 MeV/nucleon ^{3}He-rich particle events in which lower energy ions are apparently accelerated as well. Long-lived (many days) streams associated with large flares or interplanetary shocks dominate the interplanetary electron fluxes, but even at the quietest times a significant outflow of non-thermal $\gtrsim$2 keV electrons occurs. These electron phenomena are accompanied by coronal and interplanetary radio emission. High sensitivity hard X-ray measurements show that microflares, bursts with peak >20 keV fluxes 10 to 100 times smaller than observed in small solar flares, may occur as often as once every 5 min near solar maximum. The proposed Pinhole/Occulter Facility hard X-ray instrumentation provides the increase in sensitivity required to image these phenomena for the first time.

There is a wide variety of energetic electron phenomena of solar origin, observed directly in the interplanetary medium or indirectly via metric and decametric radio emission, which will produce hard X-ray emission at the Sun via electron-ion bremsstrahlung. Because of the relatively small numbers of energetic electrons involved or the low density in the corona where some of these phenomena originate, the hard X-ray fluxes are very low and up to now have not been accessible to study. Recently balloon-borne observations of very high sensitivity have discovered hard X-ray microflares, bursts with peak >20 keV fluxes a factor of 10 to 100 less than normal small flares. The relationship of these microflares to the coronal and interplanetary phenomena, if any, is unknown.

The Pinhole/Occulter Facility X-ray instrumentation will provide several orders of magnitude improvement in sensitivity as well as vastly improved spatial resolution over present-day instrumentation. The leap in sensitivity makes it possible for P/OF to study coronal phenomena in hard X rays and thus to provide the connection between phenomena observed in the interplanetary medium and at the Sun, and also to study the characteristics of hard X-ray microflares and extend their distribution to even lower flux levels. In addition it may well be possible to observe directly the region of acceleration of the electrons in flares, which presumably occurs in the low density corona. Below we discuss the various interplanetary and coronal phenomena of interest, as well as microflares and flare-related phenomena.

I. INTERPLANETARY PHENOMENA

Impulsive 2 to 100 keV Electron Events

Observations show that energetic 2 to 100 keV electrons of solar origin are continuously present in the interplanetary medium in the years near solar maximum. Small non-relativistic

solar electron events appear to be the most common type of impulsive particle emission. Figure 1 shows an example of an impulsive solar electron event (Lin, 1974; Potter, Lin, and Anderson, 1980) observed by the University of California, Berkeley, particle experiment on the ISEE-3 (International Sun Earth Explorer) spacecraft. At the time of this event the spacecraft was located in a halo orbit about the L1 Lagrange point about 10^6 km upstream of the Earth. Several important characteristics are illustrated by this figure. There is clear velocity dispersion with the fastest electrons arriving earliest, consistent with the simultaneous injection of the electrons at the Sun and nearly scatter-free propagation along the interplanetary Archimedean spiral field line to 1 AU. The rapid rise and decay at all energies confirms the lack of significant scattering. The electron distributions are highly anisotropic and beamed along the magnetic field, especially at low energies, so dips in the electron fluxes (cf. ~1140 UT in Figure 1) are observed when the magnetic field swings out of the field of view of the detector. The electron energies extend up to $\gtrsim$50 keV and down to 2 keV. Since electrons of low energies are easily lost by Coulomb scattering in the solar atmosphere, the presence of ~2 keV (the lowest energy measured) electrons indicates that most likely the coronal source of these particles is $\gtrsim$0.5 to 1 $R_\odot$ high in the solar corona, although there is also the possibility that significant energy changes have occurred for the electrons in their propagation from the Sun to 1 AU.

A total of 326 impulsive electron events were observed by ISEE-3 in the ~15 month period from August 1978 to November 1979. These events appear to fill ~60 deg in solar longitude in the interplanetary medium, so ~130 events/month must occur over the full Sun. Because the interplanetary medium is often filled with long-lived intense fluxes of electrons at these energies, small impulsive events will often not be detected. Thus the rate of occurrence of these events is probably significantly greater than estimated here.

About half of all the electron events detected do not extend in energy above ~15 keV, but almost all are observed to extend smoothly down to 2 keV, the limit of the measurement. Almost all impulsive electron events are accompanied by a solar type III radio burst observed in the interplanetary medium, i.e., at frequencies of ~30 kHz to a few MHz. On the other hand, only ~50% are associated with metric/decametric type III bursts and a minority (40%) appear to have an associated Hα flare (Solar Geophysical Data) or microwave bursts at ~3000 MHz (18%). ISEE-3 solar hard X-ray observations show that only 29% were associated with a detectable hard X-ray burst. These associations also suggest that many of these impulsive electron events probably originate at heights of ~0.5 to 1 $R_\odot$. We estimate the total energy released in electrons above 2 keV is on the order of 10^{25} ergs and the release occurs on time scales of less than a few minutes.

^{3}He-Rich Events

Recently, Reames, von Rosenvinge, and Lin (1985) reported that virtually all solar ^{3}He-rich events are associated with impulsive 2 to 100 keV electron events. Solar ^{3}He-rich events (reviewed by Ramaty et al., 1980) represent one of the most striking composition anomalies among the observed populations of solar and interplanetary energetic particles, with ^{3}He/^{4}He ratios of order unity, while the typical ratios for the solar atmosphere or solar wind are a few times 10^{-4} (Geiss and Reeves, 1972). The solar wind ^{3}He/^{4}He ratio varies but always remains below 10^{-2}, and it is uncorrelated with the occurrence of solar ^{3}He-rich events (Coplan et al., 1983). Other properties of ^{3}He-rich events include reduced ^{1}H/^{4}He ratios and enhanced abundances of Fe and other heavy elements, and a tendency to larger ^{3}He enhancements in smaller events.

With the high sensitivity of the ISEE-3 energetic particle telescopes it is possible to obtain temporal profiles with good resolution ($\lesssim$1 hr) of the ^{3}He fluxes at ~1 MeV/nucleon energy for the small ^{3}He-rich events. Figure 2 shows the 17 May 1979 events where velocity dispersion can be seen in the ^{3}He fluxes. In the lower panel the associated 2 to 100 keV impulsive electron event with its velocity dispersion can be seen. The timing of the particle onsets and maxima is shown in Figure 3, where we have plotted those times versus $1/\beta$ (the particle velocity $v = \beta c$). If particles of all velocities were released at the same time, t_0, and traveled the same distance, L, their arrival times would be related by $t = t_0 + L/\beta c$, which would be a straight line on Figure 3. The observed onset time depends upon the relative instrument sensitivity, the rise time, and the event amplitude. The ^{3}He onsets lag the time that would be expected from the electron measurements by no more than about 10 to 15 min. The traversal distance implied by the onset time of the lowest velocity ^{3}He is ~1.3 AU. This compares with ~1.25 AU for the electrons. The times of maximum of ^{3}He are also consistently later than those of electrons of the same velocity, implying a greater degree of scattering for ^{3}He in the interplanetary medium. The mean path lengths implied by the ^{3}He times of maximum are ~1.8 to 2.0 AU compared to ~1.45 AU for the electrons.

Energy spectra for the two species are shown in Figure 4. The spectral indices for the least-squares fits to a power law are 2.7 ± 0.1 and 2.7 ± 0.3 for electrons and ^{3}He, respectively. For electrons, only the region from 2.3 to 60 keV was fit because of apparent spectral changes at higher and lower energies. Note that ^{3}He and electrons have the same spectral slope over ranges of comparable particle velocities.

In the 15-month interval in 1978-79, about a dozen ^{3}He-rich events were observed with sufficient statistics to provide good temporal profiles. All of these events were accompanied by an impulsive 2 to 100 keV event with a temporal relationship similar to that shown in Figure 3. The solar associations for these ^{3}He electron events are essentially the same as for electron events in general: close association with kilometric wavelength type III bursts, small Hα subflares or no reported Hα association, very few hard X-ray bursts, and small or no soft X-ray bursts.

The close temporal associations and similar spectral slopes suggest that the same acceleration process is probably responsible for both electron and ^{3}He acceleration. The solar associations and the presence of low energy, 2 keV, electrons suggest that this acceleration probably takes place in the high corona.

A preliminary search indicates that ions of a few hundred keV total energy are accelerated at the same time as the ~1 MeV/nucleon ^{3}He and the electrons. These low energy ion fluxes are difficult to associate with an impulsive injection at the Sun because the travel time for the Sun to 1 AU is long, $\gtrsim$6 hrs, and the flux increases for ^{3}He events are small. Furthermore, there are many variations in the low energy fluxes on these same time scales, due to local interplanetary effects. Even so, for many ^{3}He impulsive electron events there are increases in the few hundred keV ion fluxes at the right time for releases simultaneous with the electrons (Figure 5). At these energies we have no information on the composition of the ions.

Thus 2 to 100 keV electrons, ~1 MeV/nucleon ^{3}He, and even lower energy ions may be accelerated together in coronal flare or flare-like events which occur at heights of 0.5 to 1 $R_\odot$. This type of acceleration differs from large flare events, where ions are accelerated to >10 MeV energies and electrons to relativistic energies, with no ^{3}He enrichment.

Long-Lived 2 to 100 keV Electron Fluxes

The ISEE-3 spacecraft observes 2 to 100 keV electron fluxes to be present in the interplanetary medium at all times. Figure 6 shows the daily minimum flux in three energy intervals: 2 to 2.3 keV electrons, 19 to 45 keV electrons and protons (but primarily electrons), and >272 keV protons. This type of plot excludes the impulsive electron events discussed above since their time scales are typically less than a few hours. It can be seen that these particle fluxes are dominated by streams which last many days. Many of these streams arise from a large solar flare event or series of such events from a single active region (Anderson, Lin, and Potter, 1982). Others appear to be dominated by the passage of an interplanetary shock (Tsurutani and Lin, 1985). Still others, generally lower intensity ones, appear to be related to type III radio burst storms observed at hectometric and kilometric wavelengths (Bougeret et al., 1985). Even at the times of the lowest counting rates the fluxes are still well above detector background, and the electrons are still streaming outward away from the Sun along the interplanetary magnetic field. Thus the Sun must be a continual source of energetic $\gtrsim$2 keV electrons. These flux levels are many orders of magnitude above the tail of the thermal 1 to 2 x 10^6 °K coronal electron distribution, so some non-thermal process must be the source. One exciting possibility is that these electrons might be a by-product of the processes which heat the solar corona.

II. OBSERVATIONS OF THE SOLAR CORONA

It is well known from radio observations that a wide variety of energetic, non-thermal phenomena occur in the solar corona. These phenomena include electron streams, both escaping (type III radio bursts) and trapped (type V and U bursts); shock wave electron acceleration (type II); acceleration and trapping of mildly relativistic electrons (type IV); and continual acceleration and storage of low energy electrons (type I bursts and continuum) (see reviews in Newkirk, 1974; Wild, Smerd, and Weiss, 1963; Kundu, 1965, 1982). Radioheliograph observations have shown that these phenomena may be highly complex, with source sizes ranging from a few arc minutes (about the resolution limit for the radio measurements) or less for type III or type I bursts to tens of arc minutes for large type II bursts. The energetic electrons that produce the radio emission will also produce hard X-ray emission via bremsstrahlung collisions with the solar coronal gas. Because the bremsstrahlung emission process is quantitatively well understood and the propagation of hard X rays through the corona is essentially unaffected by scattering and absorption, observations of coronal hard X rays can give quantitative information on the energetic electron populations in the solar corona, provided the ambient gas density in the X-ray source is known (see Brown, 1973; Lin, 1974).

Simultaneous spatially resolved hard X-ray and radio observations complement each other particularly well. Solar radio emission from the corona is believed to be generated primarily by two processes, synchrotron emission by electrons spiraling in a magnetic field and a two-step plasma wave emission process (Ginzburg and Zheleznyakov, 1958). The latter process appears to be responsible for the more common types of metric radio emission, types I, II, III, U, and possibly V. In the plasma process energetic electrons produce Langmuir plasma waves at the plasma frequency, $f_p = 9 \times 10^3 \, n^{1/2}$ Hz, where n is the plasma density in cm^{-3}. These waves then scatter off ion density fluctuations or low frequency waves, or off other Langmuir waves to produce electromagnetic radiation at the plasma frequency, f_p (fundamental), or twice the plasma frequency, $2f_p$ (2nd harmonic), respectively. The production of radio waves depends on the details of the energetic electron distribution function – whether it is unstable to the coherent generation of plasma waves – and also on the plasma wave to electromagnetic wave conversion process. The intensity of the radio emission, its apparent size, and its location in the corona will

be modified by scattering and absorption in the corona. It is difficult, therefore, to obtain quantitative information on the energetic electron population from the radio emission. On the other hand the ambient coronal density is closely related to the frequency of the observed radiation in the plasma wave emission process. Furthermore, radio waves, whatever the generation mechanism, cannot propagate through the coronal plasma unless their frequency is above the local plasma frequency. Thus, radio observations can provide the coronal density information needed for quantitative interpretation of the hard X-ray observations.

Hard, >20 keV, X-ray bursts are commonly observed during the impulsive phase of flares, but this emission most likely originates in the high density, $n \gtrsim 10^{10}$ cm^{-3}, chromosphere (see Kane, 1974, for review). A few hard X-ray events have been interpreted as X-ray emission from the corona because the associated flare was believed to be well behind the solar limb (Hudson, 1978; Hudson, Lin, and Stewart, 1982). Most coronal phenomena will produce a level of bremsstrahlung X-ray fluxes too low for detection by present-day solar hard X-ray instrumentation, because both the ambient densities in the solar corona and the number of energetic electrons involved are low. P/OF, with its coronagraph and hard X-ray imaging instruments, together with ground-based radioheliographs, would be ideal for quantitative studies of the coronal phenomena. Below we describe a few of the many scientific topics which can be investigated.

Type III Bursts

Type III radio bursts are the most common type of impulsive non-thermal phenomena at the Sun. They are characterized by a rapid frequency drift from high to low frequencies (Wild, Smerd, and Weiss, 1963). Simultaneous in situ particle and low-frequency radio observations from spacecraft at 1 AU have shown that type III bursts are excited by ~2 to 100 keV electrons which escape from the Sun following an impulsive acceleration (Lin, Evans, and Fainberg, 1973, 1981a). The observed starting frequencies for type III bursts extend down to ~100 to 500 MHz or greater, corresponding to initial ambient densities, n, of $\approx 10^8$ to 10^9 cm^{-3}. Most type III bursts are unaccompanied by flares or soft X-ray increases (based on OSO-7 soft X-ray observations). Hard X-ray emission has been observed for some flare-associated type III bursts, but these tend to occur for only ~25% of the most intense bursts with very high starting frequencies (i.e., high densities). In these the X-ray and radio emissions sometimes show coincident time structure (see Figure 7). The interplanetary measurements indicate the energetic electron spectrum for type III events extends down to $\lesssim 2$ keV (Figure 4). The total number of electrons escaping into the interplanetary medium is estimated to be $N(>5 \text{ keV}) \approx 5 \times 10^{34}$ in a typical type III event. At the Sun the radio event may comprise a number of individual bursts, quasi-periodically spaced.

As an example we calculate the X-ray emission for a type III burst under the model assumption of instantaneous acceleration of the electrons and escape from the Sun without significant losses. Suppose at t = 0, $N(>E_0)$ electrons were accelerated with a power-law energy spectrum, $dN/dE = AE^{-\delta}$, and released from a region of ambient density n_0. The ambient density $n(cm^{-3})$ of the region the electrons pass through is given by the frequency f(MHz) of the type III emission, if we know whether the emission is at the fundamental or the 2nd harmonic emission. The observed frequency drift rate then determines the change in ambient density as a function of time. Alvarez and Haddock (1973) find that between 550 MHz and 75 kHz the average $df/dt = 0.01\ f^{1.84}$ MHz/s. Integrating, we obtain f(t) and therefore n(t):

$$n(t) = n_0(1 + atn_0^{0.42})^{-2.38}$$

where $a = 2.9 \times 10^{-4}$ for harmonic and 1.6×10^{-4} for fundamental emission. The X-ray emission is then given by

$$\frac{dJ}{d(h\nu)} = \frac{A\, n_j (h\nu)^{-\delta-1/2}}{1.2 \times 10^{42}\, (\delta + 1/2)\, (\delta - 1/2)^2\, B(\delta, 3/2)} \quad ,$$

where B is the beta function. The computed temporal variation is given in Figure 8 for a variety of n_0 and fundamental and harmonic radio emission.

For typical type III events the detailed temporal and spatial structure can be resolved by P/OF. These observations will provide information on:

(i) The characteristics of the acceleration processes and the location of the acceleration region relative to other coronal structure. Comparison of type III and flare events should help determine whether two different acceleration processes are involved.

(ii) The characteristics of electron propagation in the solar corona. This is important because energetic electrons appear to fill an ~60 deg FWHM cone at 1 AU while type III burst sizes are much smaller near the Sun.

(iii) The magnetic field structure of the corona. The type III electrons are tracers of the magnetic field lines. For most type III bursts the radio location appears close to the flare or active region (Duncan, 1977) so these observations may show how magnetic fields from different areas of the Sun intermix in the corona.

(iv) The characteristics of the type III emission mechanism. Is the emission generated only in favored "core" regions (Smith and Nicholson, 1978)? Is the near-Sun emission at the fundamental or harmonic or both (Rosenberg, 1975)? Do the electrons begin generating radio emission immediately or must they travel some minimum distance to obtain an unstable distribution from velocity dispersion? Do the electrons lose energy rapidly through beam-plasma interactions near the Sun?

Other Coronal Radio Phenomena

Type I, V, and U bursts also occur very commonly. The origins of these phenomena are less well understood than type III bursts. Type I radio bursts are superimposed on noise storm continua. They often show frequency drifts in both senses with drift rates ~1/4 to 1/2 of type III's. Thus it is hypothesized that electrons of a few to 10 keV energy are the exciters of this radiation via the plasma mechanism. Type V and U's appear to be closely related to type III bursts, possibly just due to the electron stream traversing peculiar magnetic field configurations. Type V bursts follow type III bursts, and III-V bursts are closely correlated to observed flare hard X-ray impulsive bursts (Stewart, 1978).

Type II and IV bursts are rarer, occurring an average of several times per month. These phenomena are particularly interesting in that they appear to be associated with coronal acceleration of ions and relativistic electrons which occur for some large flares. The hard X-ray emission from type II bursts may have been observed for some flares beyond the solar limb (Frost and Dennis, 1971; Hudson, 1978; Hudson, Lin, and Stewart, 1982). Type IV bursts are apparently due to synchrotron radiation. Comparison of radio and X-ray spatial observations can be used to obtain information on the magnetic field in the corona. Type II radio bursts are associated with shock waves, but it is not clear how the emission is produced. One hypothesis is that electrons accelerated at the shock generate the radio emission via the plasma-wave process. Supporting this hypothesis is the observation of "herringbone" structure, fast drift bursts similar to type III's

which appear to originate at the shock. These III-like structures are observed to extend to low frequencies (Cane et al., 1981). Simultaneous coronal X-ray and radio observations would be useful for studying the acceleration processes in the shock.

Particle Storage and Continual Acceleration in the Corona

There exists substantial evidence for the continual acceleration and/or storage of energetic electrons in the corona. Radio continua at meter wavelengths, such as noise storms and stationary type IV events, last hours to days (see Kundu, 1965, for review). The interplanetary medium, even at the quietest times, contains a population of 2 to 100 keV electrons, presumably of solar origin. Much more intense fluxes of electrons appear in active region-associated particle streams which can last for several solar rotations (Anderson, 1969). Electron and proton fluxes from large solar flare events last for several weeks even though the time scale for the solar wind to sweep these particles out of the inner solar system is ~4 days (see McCracken and Rao, 1970, for review).

Coronal X-ray observations can answer several important questions:

(i) Are energetic electrons being stored in the corona? Where and for how long? What are the loss processes for these particles?

(ii) Is there acceleration of electrons in the absence of flares or other transient phenomena? Perhaps the same processes which heat the corona also continuously accelerate electrons.

(iii) Are energetic electrons stored in the corona a viable energy source for flares?

Using the electron energy loss rate in ionized hydrogen (Trubnikov, 1965) we find that the e-folding energy loss time is given by

$$t_e \approx 10^8 \, E^{3/2} \, n^{-1} \quad .$$

Thus electrons of 5 and 20 keV energy must be stored at densities of $n = 10^4$ to 10^5 cm^{-3}, respectively, for 1-day e-folding loss times. Spatial and spectral observations of storage regions will give detailed information on the continual acceleration, storage, and loss processes. For example, if Coulomb collisions are the dominant loss process, the electron energy spectrum will harden between fresh accelerations. By utilizing interplanetary particle observations to estimate the electron escape term and solving the continuity equation for simple models, it may also be possible to obtain information on continuous acceleration processes in the absence of flares.

It is estimated that $\sim 10^{35}$ to $10^{36} > 10$ keV electrons are accelerated during flares. If the observed flare impulsive hard X-ray emission is produced by thin target processes, i.e., without significant losses for the electrons (Datlowe and Lin, 1973), then these electrons must be stored high in the corona since fewer than 1% are observed to escape. The stored electrons presumably produce X-ray emission at a level too low to be observed by present-day instrumentation, but this level of X-rays should be easily observed and imaged by P/OF. Since a small flare has a total energy output of $\sim 10^{29}$ ergs, equivalent to $\sim 10^{36}$ keV electrons, P/OF can provide conclusive evidence for or against the hypothesis that energetic particles slowly accelerated and stored in the corona are a viable energy source for flares (Elliott, 1969).

III. MICROFLARES

The Sun exhibits a broad spectrum of transient phenomena with total energy release substantially less than flares. Transient soft X-ray brightenings are observed in a continuum of intensities from flares down to tiny X-ray bright points. It is not known how similar these less energetic transient phenomena are to flares – whether they also involve significant particle acceleration or whether below some total energy released they are basically thermal in character.

High sensitivity hard X-ray observations of the Sun, made with balloon-borne instrumentation designed for detecting cosmic hard X-ray sources, provide an indication of what might be observed and imaged by P/OF. On 27 June 1980 the Sun was observed for ~141 min by a combination of a 300 cm^2 NaI/CsI phoswich scintillator and 50 cm^2 array of germanium detectors, both collimated and surrounded with active anticoincidence shields (Lin et al., 1981b; 1984). Figure 9 shows 16.384 s averages of the 22 to 23 keV count rate of the balloon phoswich scintillator for the solar observing periods. To provide a measure of the sensitivity of this detector, we note that the Crab nebula increases the 22 to 33 keV count rate by ~5 counts/s. The count rate of the 5 to 6 keV channel of the soft X-ray proportional counter detectors of ISEE-3 is shown above.

Besides the large flare (1614 to 1632 UT) there are at least four clearly recognizable bursts with count rate increases of $\gtrsim$5 counts/s (1559, 1950, 1958, and 2032 UT). These tend to occur on the rising portion of their associated soft X-ray bursts, as is often observed for flares. On closer examination, many smaller bursts can be seen, for example, at 1532, 1545, 1605, 1939, 1953, and 2058 UT. We have made a detailed search for additional small bursts. In 141 min of solar observing, a total of 25 separate increases, including those listed above, were detected above the 3σ level. This compares with three to four events expected for this period of time from purely statistical fuctuations. Most of these hard X-ray microflares detected above the 3σ level in the solar observing periods appear to have an associated 5 to 6 keV soft X-ray burst and vice versa; however, the ratio of 22 to 23 keV flux to 5 to 6 keV flux varies by more than one order of magnitude.

The temporal structure of the four largest microflares is shown in Figure 10. There is some evidence that these small bursts are composed of smaller, more "elementary" bursts. The events at 1950 and 1958 consist of individual bursts of 1 to 2 s FWHM duration. The bursts at 1559 and 2032 UT could be deconvolved into groups of elementary bursts of the same 1 to 2 s FWHM duration.

Accurate energy spectra, as measured by the germanium detector array for the four largest microflares, are shown in Figure 11. The spectra are best fit by power laws,

$$dJ/dE = AE^{-\gamma} ,$$

with slopes $\gamma \approx 4$ to 6. The spectra extend out to ~70 to 80 keV for the largest events. Preliminary comparisons with the ISEE-3 soft X-ray data indicate that the power-law spectrum often extends down into the energy range (5 to 14 keV) of the proportional counter detector.

Figure 12 shows the integral distribution of events versus the maximum 20 keV flux in the burst. For comparison, the distribution obtained in the previously published survey (Datlowe, Elcan, and Hudson, 1974) is also shown. We emphasize here that the balloon data on occurrence

rates are based on only ~2 hours of observation, at a time close to solar maximum, while the OSO-7 observations span an 8-month period several years after solar maximum. The slopes of the two distributions can be seen to be the same, about -1; however, the balloon data extend the flux range down by more than one order of magnitude. There is no evidence for flattening of the distribution down to flux levels of 10^{-2} (cm^2 s keV)$^{-1}$. The rate of occurrence during the balloon observations is about a factor of 3 greater than the OSO-7 average rate.

During this observation period solar hard X-ray bursts occurred at a rate far higher than that for reported Hα flares of radio bursts. Furthermore, the integral number of bursts continues to increase with decreasing flux, indicating that with a lower threshold even more bursts would be observed. Already at this threshold level the numbers of hard X-ray and soft (~5 keV) X-ray bursts are essentially comparable. These observations suggest that a common property of transient energy releases by the Sun is the acceleration of electrons to energies above ~20 keV.

The total energy combined in these electrons can be computed under the normal assumption of thick target, i.e., that the electrons lose their energy primarily through Coulomb collisions (Brown, 1973; Lin, 1974). The total energy in >20 keV electrons ranges from a few times 10^{26} to ~10^{28} ergs for the four largest events shown in Figure 2. The average rate of energy deposition by greater than 20 keV electrons from all the bursts above a flux threshold of 10^{-2} (cm^2 s keV)$^{-1}$ is ~10^{24} ergs/s. These energy figures will increase by about one order of magnitude for every factor of 2 lower in energy the power-law electron spectrum extends. Preliminary analysis of the ISEE-3 data suggests that the electron spectrum extends to at least ~10 keV, and perhaps 5 keV. Furthermore, the number of events continues to increase as the flux threshold decreases. Thus the total rate of energy released in electrons producing these small hard X-ray bursts may be substantial, perhaps even comparable to the 10^{27} ergs/s rate of heating of the active corona.

IV. P/OF HARD X-RAY OBSERVATIONS

We have used the estimates of the numbers of electrons (vertical scale of Figure 13) from the interplanetary observations as a basis for computing the hard X-ray emission from the corona for various phenomena. The numbers of electrons observed at 1 AU will constitute a lower limit to those at the Sun since electrons could be lost by various processes in propagating to 1 AU. The electrons will produce X rays via the electron-ion bremsstrahlung process in the solar corona. Since bremsstrahlung is a collisional process the X-ray flux will depend on the ambient ion density (horizontal scale of Figure 13).

For the long-lived streams the electron population in the corona are estimated assuming a steady-state outflow into a region whose cross section expands as r^2. The time scale for each phenomenon is also indicated. Those phenomena such as flares or microflares, which have been observed in hard X rays, are indicated by the diagonal regions. An estimate of the sensitivity of the proposed hard X-ray imaging instrumentation for P/OF is superimposed. It can be seen that essentially all the microflare and flare phenomena can be imaged by P/OF at appropriate time scales. P/OF will also provide a first look at coronal phenomena from long-lived streams to flare-related impulsive phenomena.

Finally it should be emphasized that P/OF may be able to locate and image the region of acceleration of electrons in flares, rather than the region where the electrons lose most of their energy. Presumably the acceleration occurs in a low density, $n_i \lesssim 10^9$ cm^{-3}, coronal region, perhaps at the top of the flare loop. If the loop length is a few x 10^4 km, then electrons will

travel to the footpoints in a few tenths of a second. With the sensitivity of P/OF it may be possible to image the acceleration region and follow the propagation of the energetic electrons in the flare loop in the few tenths of a second prior to the impact of the electrons in the footpoints. The identification of the acceleration region would then permit the determination of the physical parameters in the region by other instruments such as the coronagraphs and soft X-ray telescopes.

Acknowledgments. This research was supported in part by NASA grants NAG 5-376, NAGW-516, and NGL-05-003-017, and NSF grant ATM-8402231.

REFERENCES

Alvarez, H. and Haddock, F. T., 1973, *Solar Phys., 29,* 197.
Anderson, K. A., 1969, *Solar Phys., 6,* 111.
Anderson, K. A., Lin, R. P., and Potter, D. W., 1982, *Space Sci. Rev., 32,* 169.
Bougeret, J. L., Lin, R. P., Fainberg, J., and Stone, R. G., 1985, *Astron. Astrophys.,* in press.
Brown, J. C., 1973, *Solar Phys., 31,* 143.
Cane, H. V., Stone, R. G., Fainberg, J., Stewart, R. T., Steinberg, J. L., and Hoang, S., 1981, *Geophys. Res. Lett., 8,* 1285.
Coplan, M. A., Ogilvie, K. W., Boschler, P., and Geiss, J., 1983, *Solar Wind Five,* NASA Conference Publication 2280, Washington, D.C., p. 591.
Datlowe, D. W., Elcan, M. J., and Hudson, H. S., 1974, *Solar Phys., 39,* 155.
Datlowe, D. W. and Lin, R. P., 1973, *Solar Phys., 32,* 459.
Duncan, R. A., 1977, *Proc. Astron. Soc. Austral., 3,* 154.
Elliott, H., 1969, in *Solar Flares and Space Research,* eds. C. deJager and Z. Svestka, North-Holland Publ. Co., Amsterdam, p. 356.
Frost, K. J. and Dennis, B. R., 1971, *Astrophys. J., 165,* 655.
Geiss, J. and Reeves, H., 1972, *Astron. Astrophys., 18,* 126.
Ginzburg, V. L. and Zheleznyakov, V. V., 1958, *Soviet Astron., AJ2,* 653.
Hudson, H. S., 1978, *Astrophys. J., 224,* 235.
Hudson, H. S., Lin, R. P., and Stewart, R. T., 1982, *Solar Phys., 75,* 245.
Kane, S. R., 1972, *Solar Phys., 27,* 174.
Kane, S. R., 1974, in *Coronal Disturbances,* ed. G. Newkirk, Jr., IAU Symp. 57, D. Reidel, Dordrecht-Holland, p. 105.
Kundu, M. R., 1965, *Solar Radio Astronomy,* John Wiley, New York.
Kundu, M. R., 1982, *Rep. Prog. Phys., 45,* 1435.
Lin, R. P., 1974, *Space Sci. Rev., 16,* 189.
Lin, R. P., Evans, L. G., and Fainberg, J., 1973, *Astrophysical Letters, 14,* 191.
Lin, R. P., Potter, D. W., Gurnett, D. A., and Scarf, F. L., 1981a, *Astrophys J., 251,* 364.
Lin, R. P., Schwartz, R. A., Pelling, R. M., and Hurley, K. C., 1981b, *Astrophys. J. (Letters), 251.* L109.
Lin, R. P., Schwartz, R. A., Kane, S. R., Pelling, R. M., and Hurley, K. C., 1984, *Astrophys. J., 283,* 421.
McCracken, K. G. and Rao, U. R., 1970, *Space Sci. Rev., 4,* 155.
Newkirk, G., Jr. (ed.), 1974, *Coronal Disturbances,* D. Reidel, Dordrecht, Holland.
Potter, D. W., Lin, R. P., and Anderson, K. A., 1980, *Astrophys. J. (Letters), 236,* L97.
Ramaty, R., and 10 co-authors, 1980, in *Solar Flares, A. Monograph from the Skylab Solar Workshop II,* ed. P. A. Sturrock, Colorado Assoc. University Press, p. 117.
Reames, D. V., von Rosenvinge, T. T., and Lin, R. P., 1985, *Astrophys. J.,* in press.
Rosenberg, H., 1975, *Solar Phys., 42,* 247.
Smith, D. F. and Nicholson, D. R., 1978, preprint, Dept. of Astro-Geophysics, Univ. of Colorado.
Stewart, R. T., 1978, *Solar Phys., 58,* 121.
Trubnikov, B. A., 1965, *Rev. Plasma Phys., 1,* 105.
Tsurutani, B. and Lin, R. P., 1985, *J. Geophys. Res., 90,* 1.
Wild, J. P., Smerd, S. F., and Weiss, A. A., 1963, *Ann. Rev. Astron. Astrophys., 1,* 291.

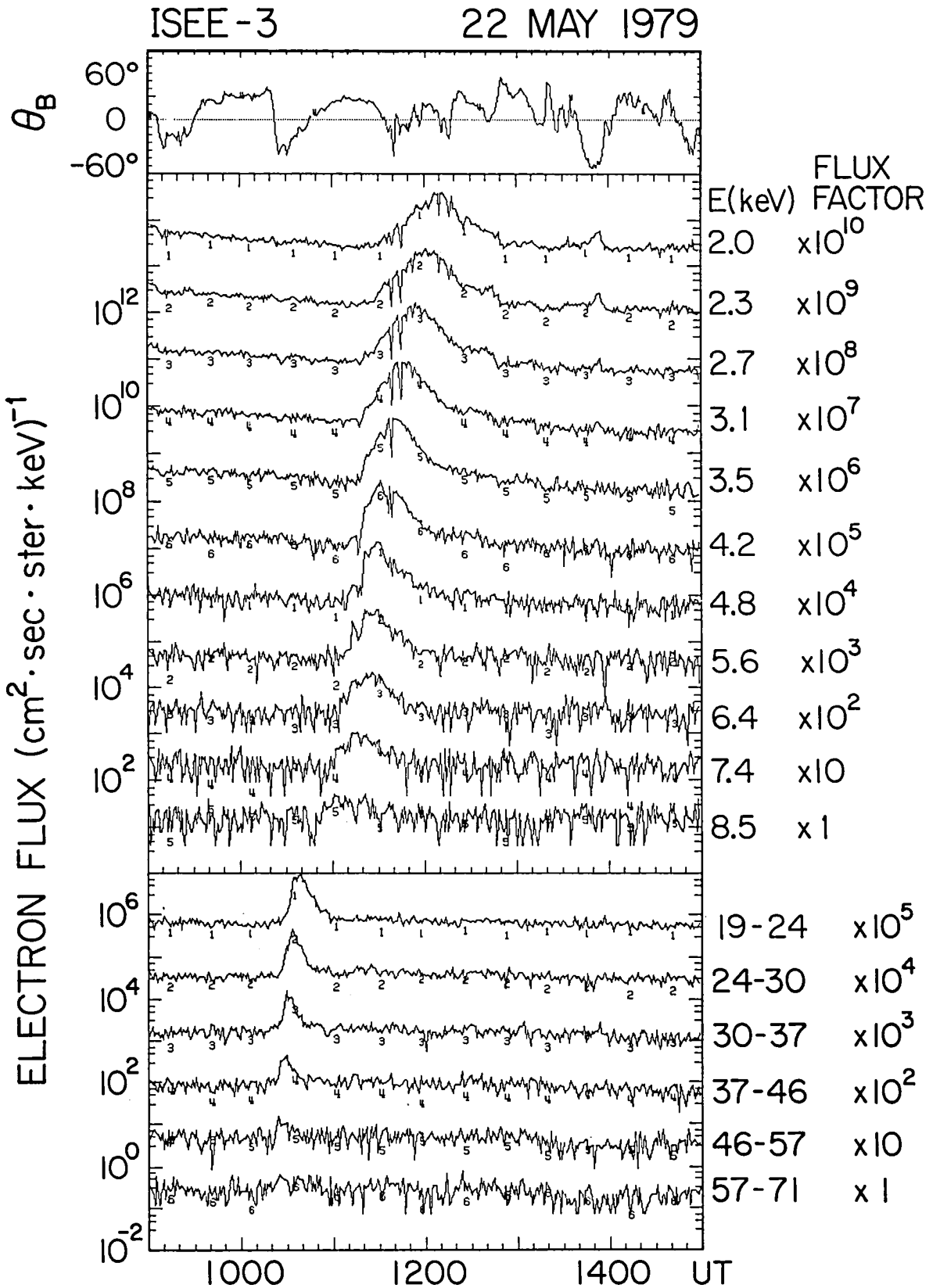

Figure 1. An impulsive solar electron event observed by the ISEE-3 spacecraft. Note the rapid-rise rapid-fall profiles and the clear velocity dispersion. The top panel shows the angle of the interplanetary magnetic field direction to the ecliptic plane.

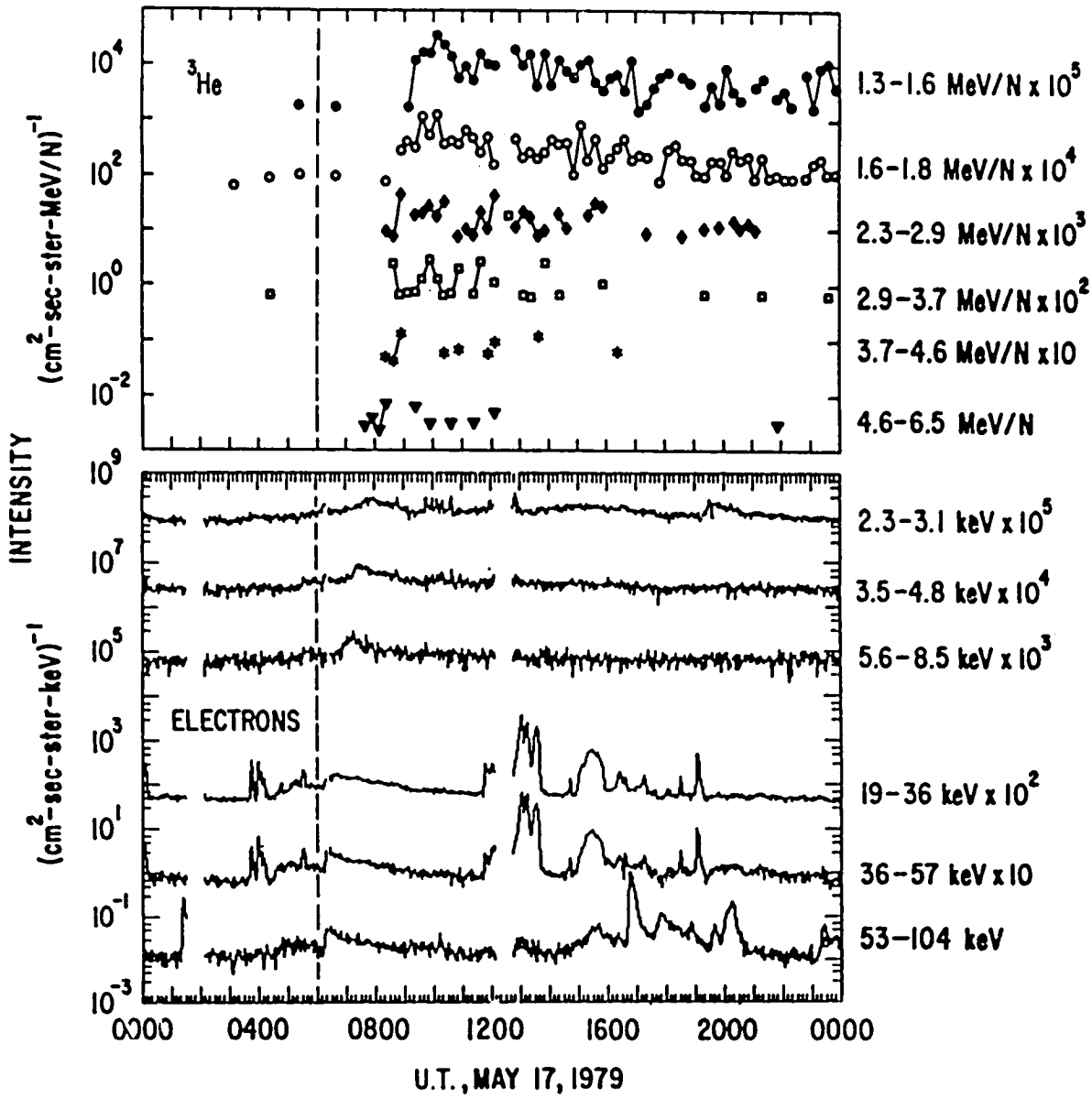

Figure 2. Time histories of the intensities of ^{3}He and electrons of the indicated energy during 17 May 1979 (from Reames, von Rosenvinge, and Lin, 1985). The appearance of the plots differs partly because of the absence of continuous background fluxes for ^{3}He. The lowest isolated points for each energy of ^{3}He represent one particle per 15-min averaging period. The rapidly varying bursts (at ~0400 UT and ~1200 UT) observed in the higher, >19 keV, energy electron channels are due to particles from the Earth's bow shock. The 53 to 104 keV channel also responds to solar X-rays (~0130, 1630 to 2030, and 2330 UT). The dashed vertical line indicates the time of the Type III solar radio burst. Intensity scale factors are shown to the right of the energies.

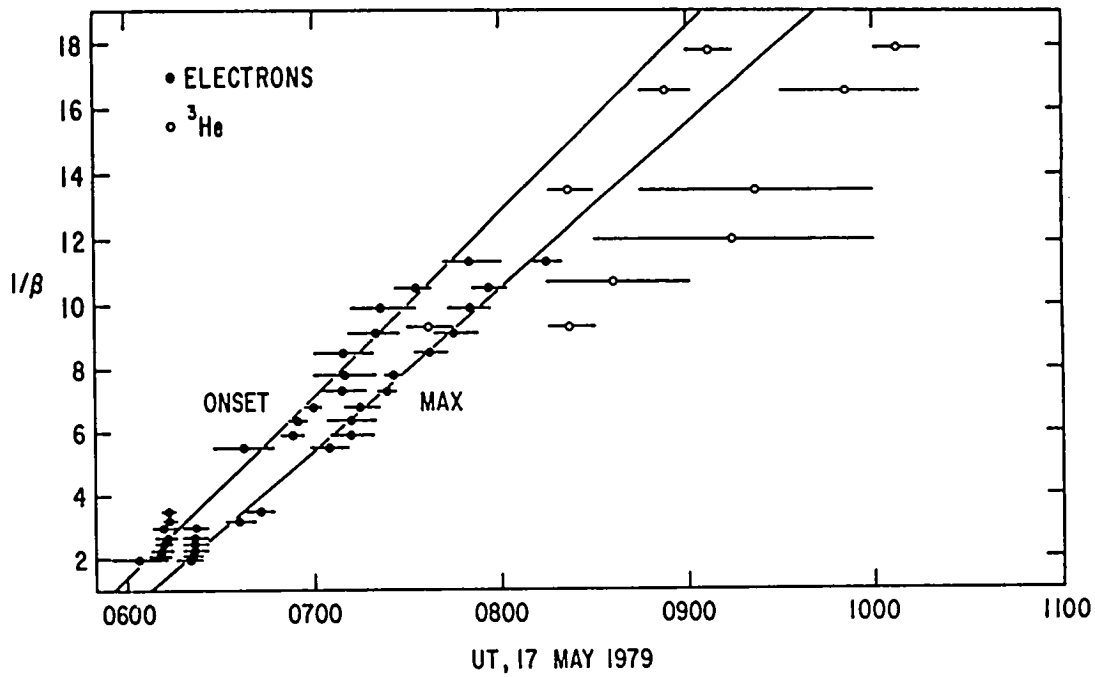

Figure 3. Time of onset and peak flux for particles plotted versus $1/\beta$ where $v = \beta c$ in the particle velocity (from Reames, von Rosenvinge, and Lin, 1985). The lines represent least-squares fits to the electron data only.

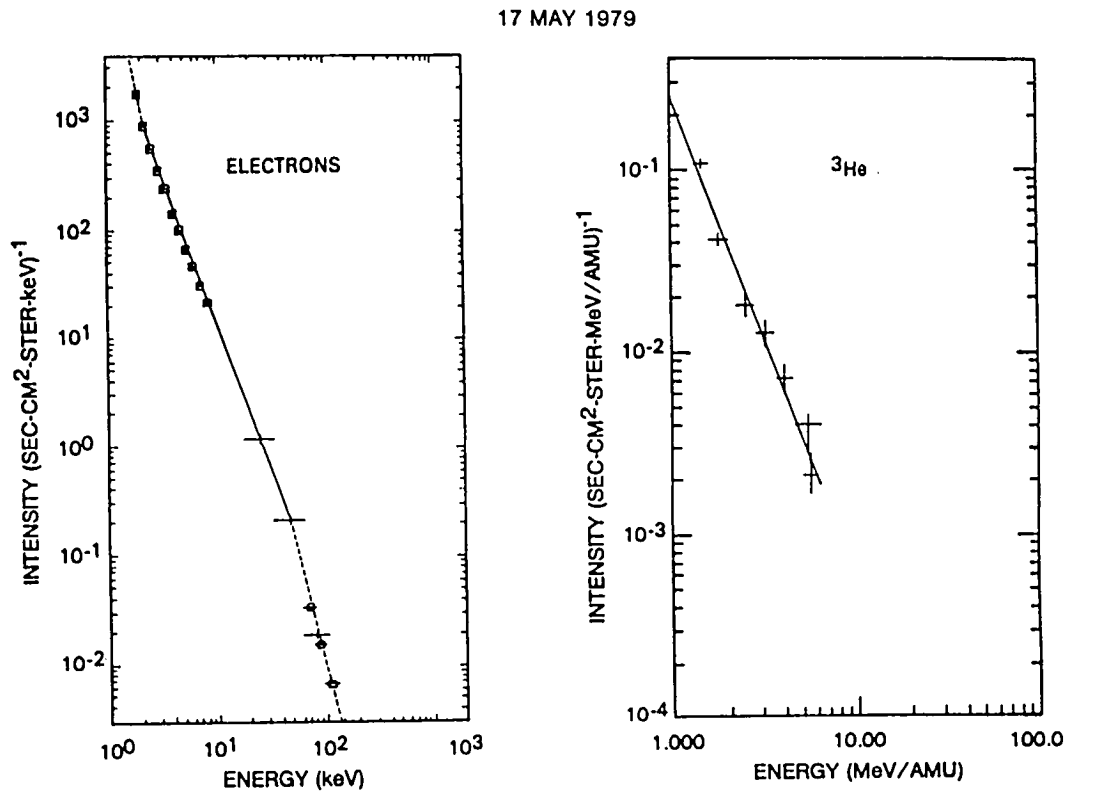

Figure 4. Event-averaged energy spectra for electrons and ^{3}He in the 17 May 1979 event (from Reames, von Rosenvinge, and Lin, 1985). Lines through the data are least-squares fit lines to power-law spectra with resulting spectral indices 2.7 ± 0.1 for electrons and 2.7 ± 0.3 for ^{3}He. The electron fit was confined to the 2.5 to 60 keV region.

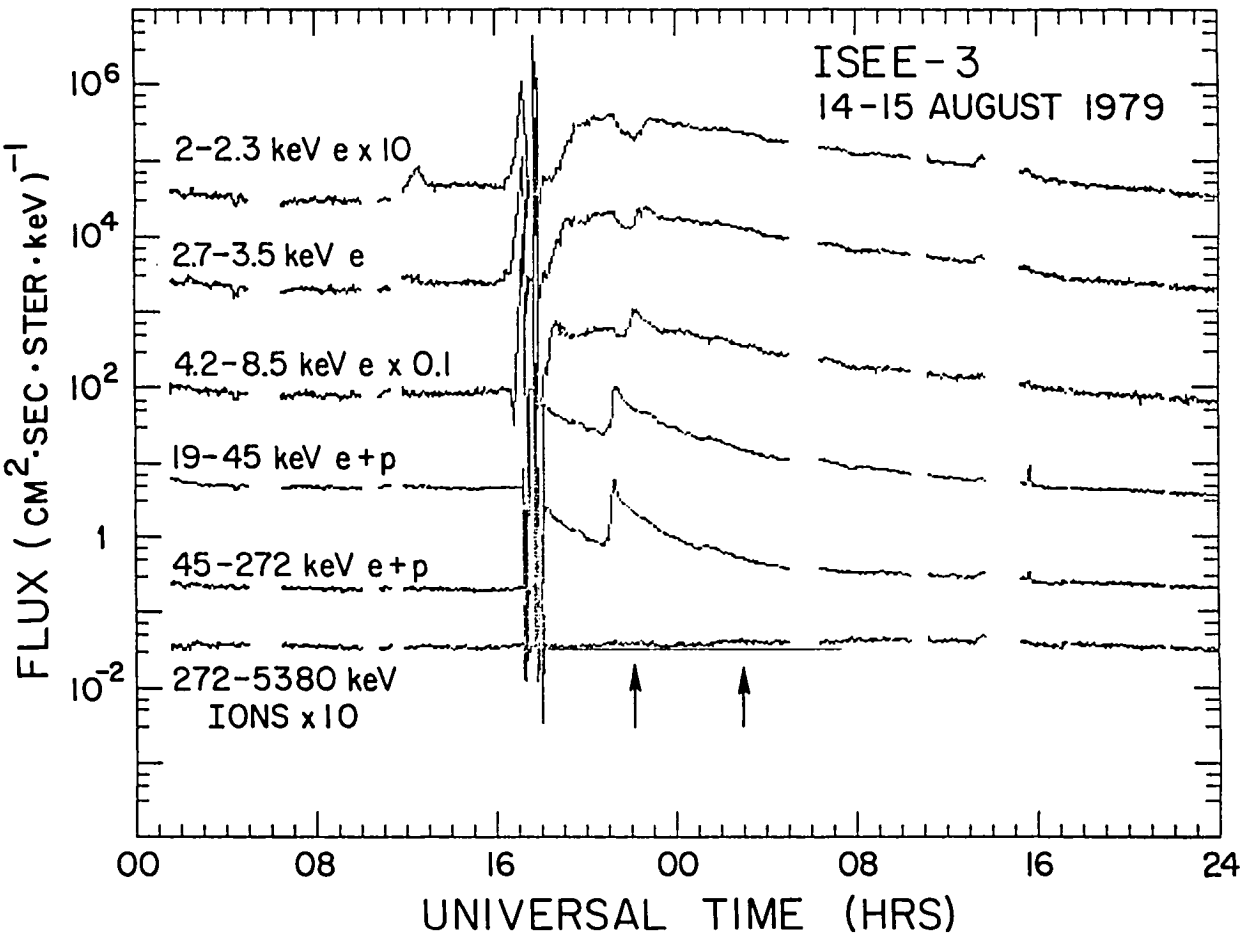

Figure 5. A pair of impulsive electron events which are closely associated with ^{3}He increases. The bottom trace shows >272 keV protons. The two barely visible small increases about 6 hours after each electron injection may be due to a few hundred keV ions also accelerated at the same time. A calibration cycle occurred at 1700 to 1800 UT on 14 August.

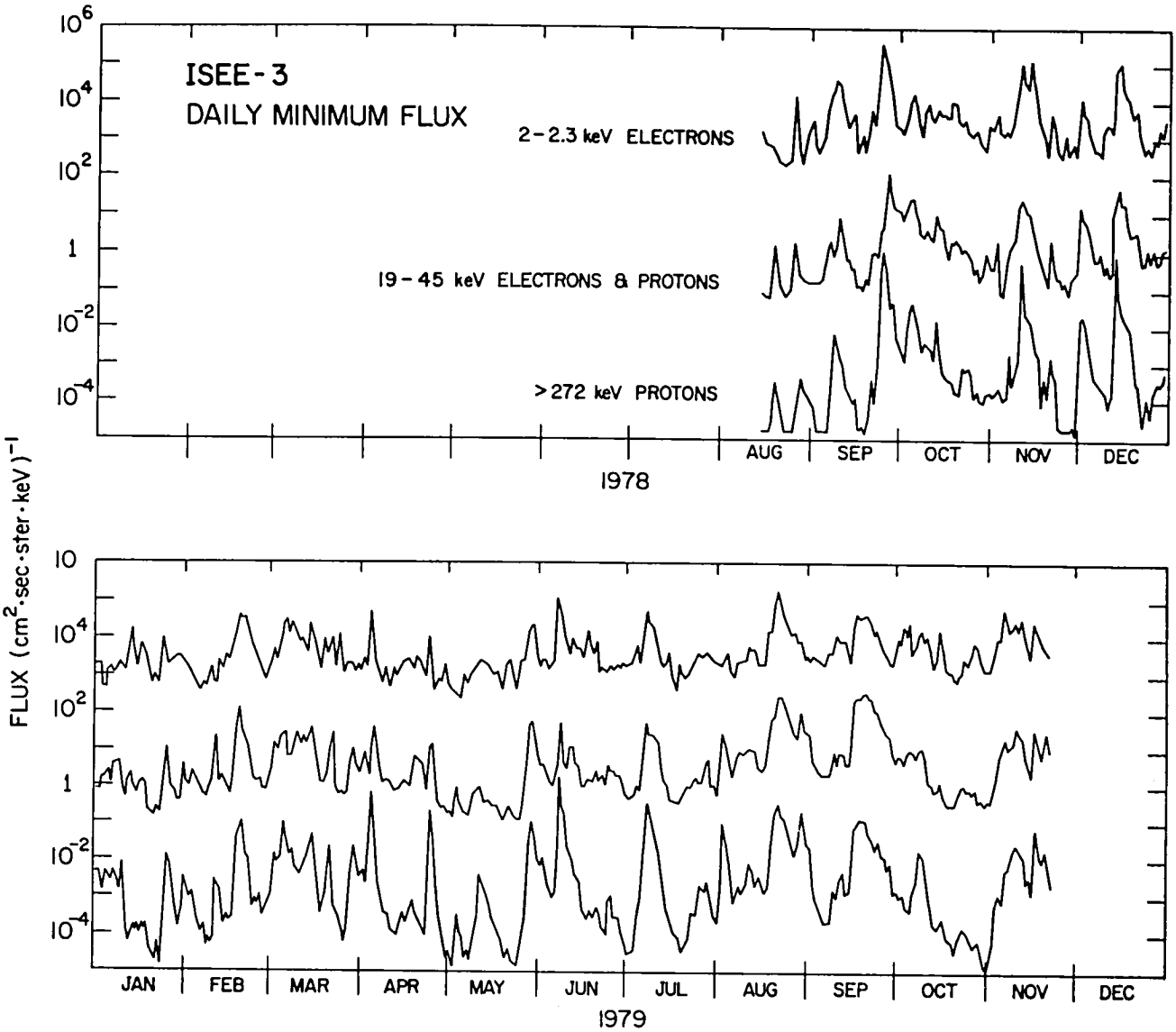

Figure 6. Plotted here are the minimum flux levels for each day of 2 to 2.3 keV electrons, 19 to 45 keV electrons and protons, and >272 keV protons, for August 1978 to November 1979. The fluxes are dominated by long-lived streams, but even at the quietest times there are significant fluxes of electrons.

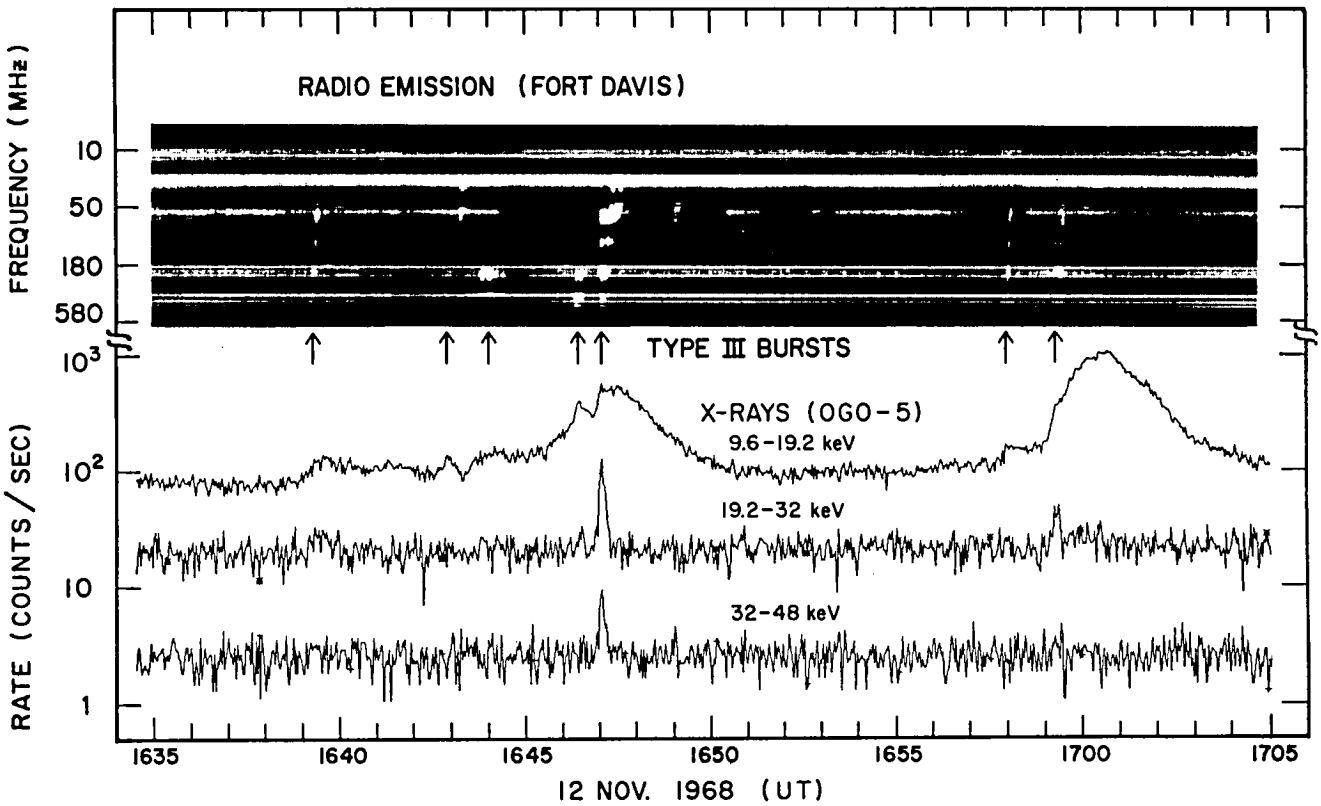

Figure 7. A series of type III bursts in time coincidence with non-thermal X-ray emission (from Kane, 1972). For every type III burst in this series there is a corresponding increase in X-ray flux.

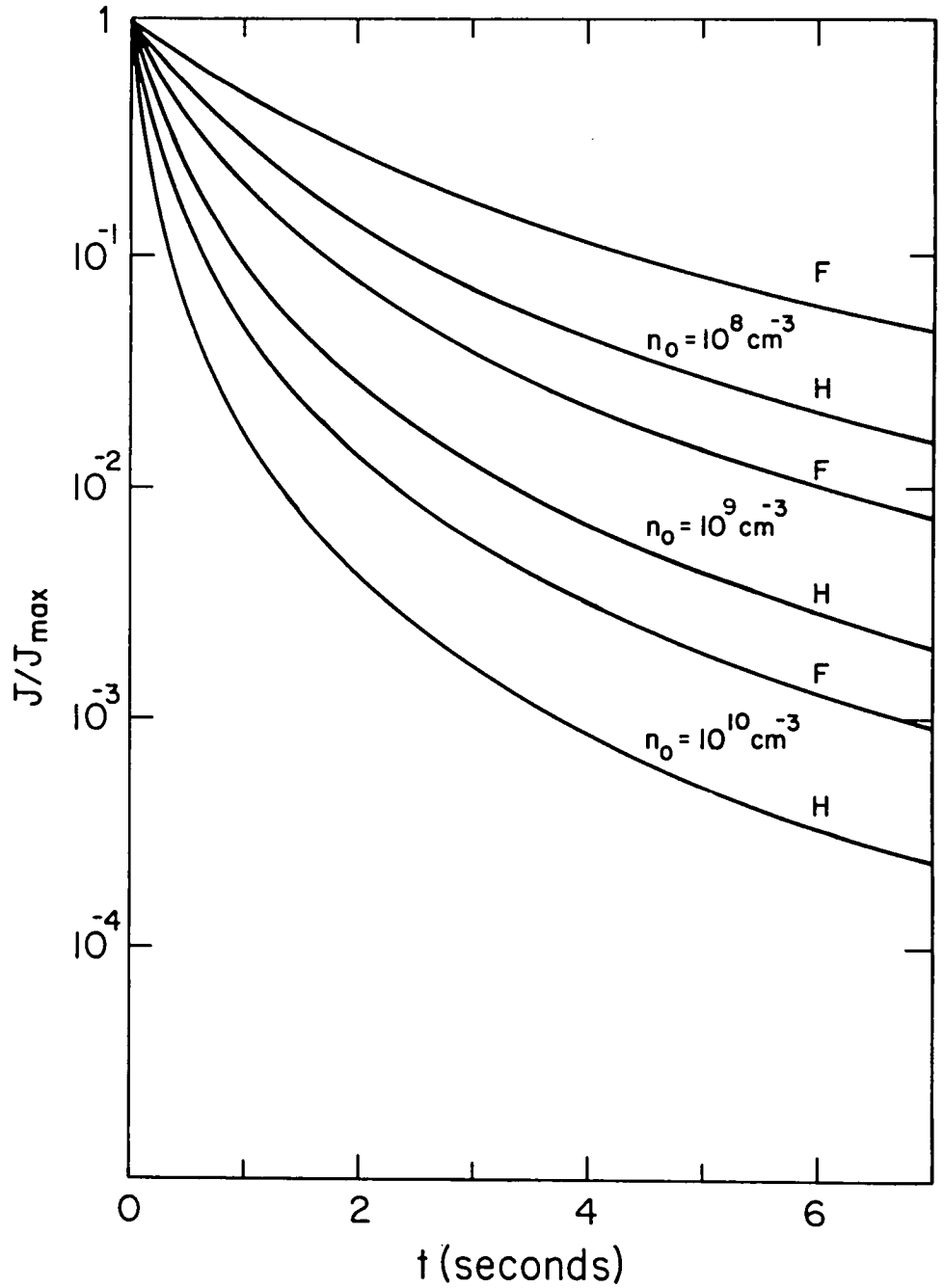

Figure 8. The time profiles for the coronal hard X-ray emission from a type III radio burst, computed under the assumption of instantaneous acceleration and escape of the electrons without significant energy loss. The curves are computed for different starting frequencies and normalized to the maximum flux. F and H denote interpretation of the radio emission as fundamental or harmonic.

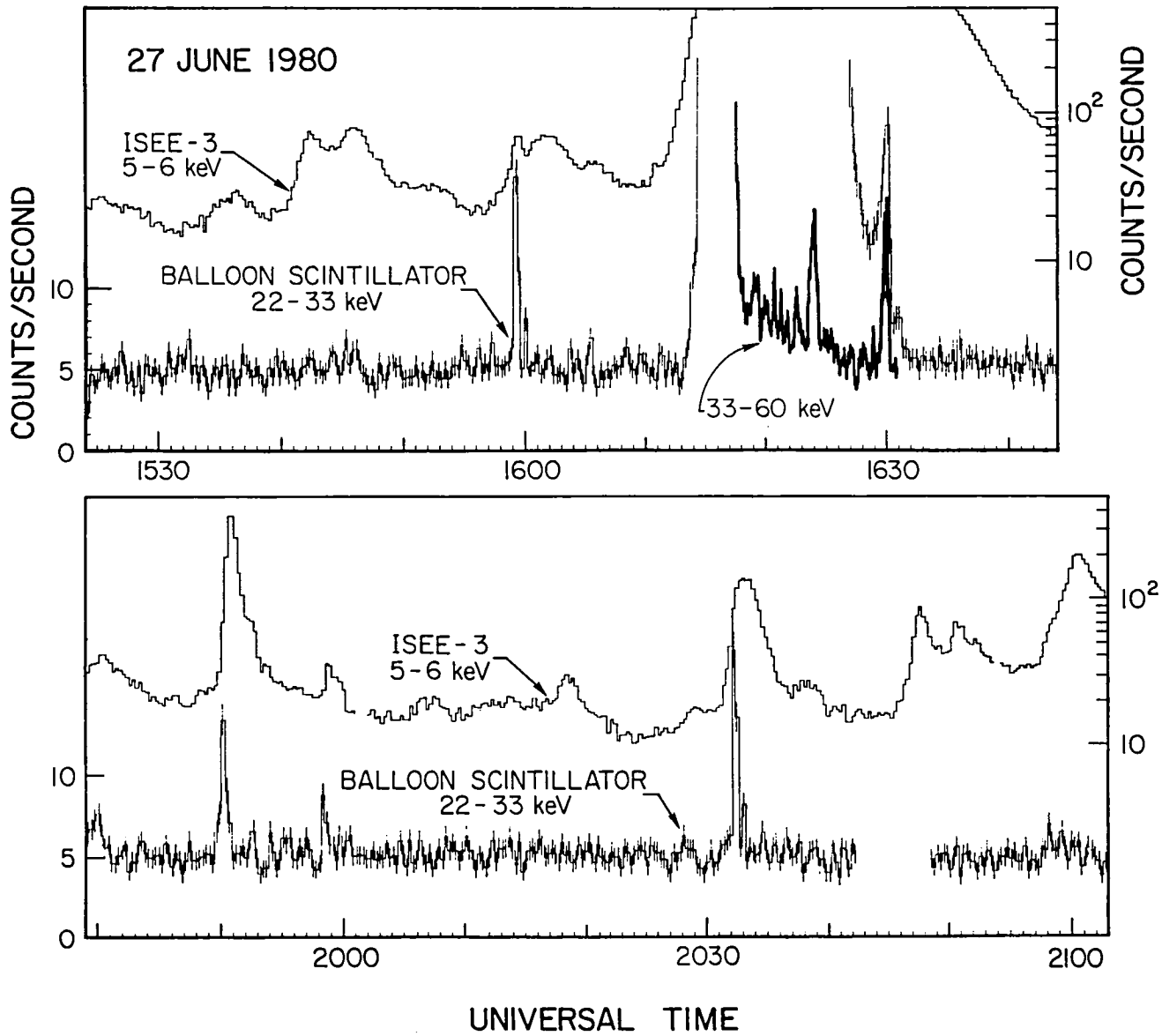

Figure 9. The 22 to 33 keV count rate of the NaI/CsI phoswich scintillation detector for the two solar observing periods is shown here together with the soft X-ray count rate for the ISEE-3 spacecraft (from Lin et al., 1984). Between 1618 and1631 UT, the 33 to 60 keV count rate (thick line) is shown as well.

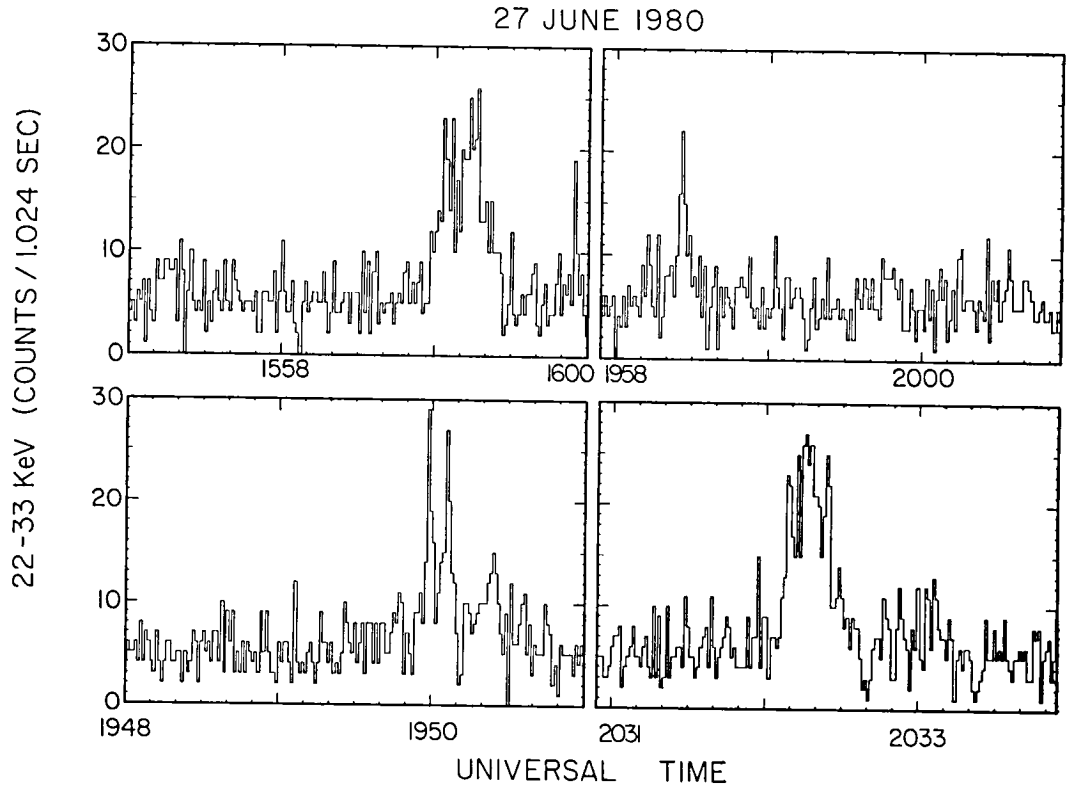

Figure 10. The four largest hard X-ray microflares are shown here at 1.024 s resolution (from Lin et al., 1984).

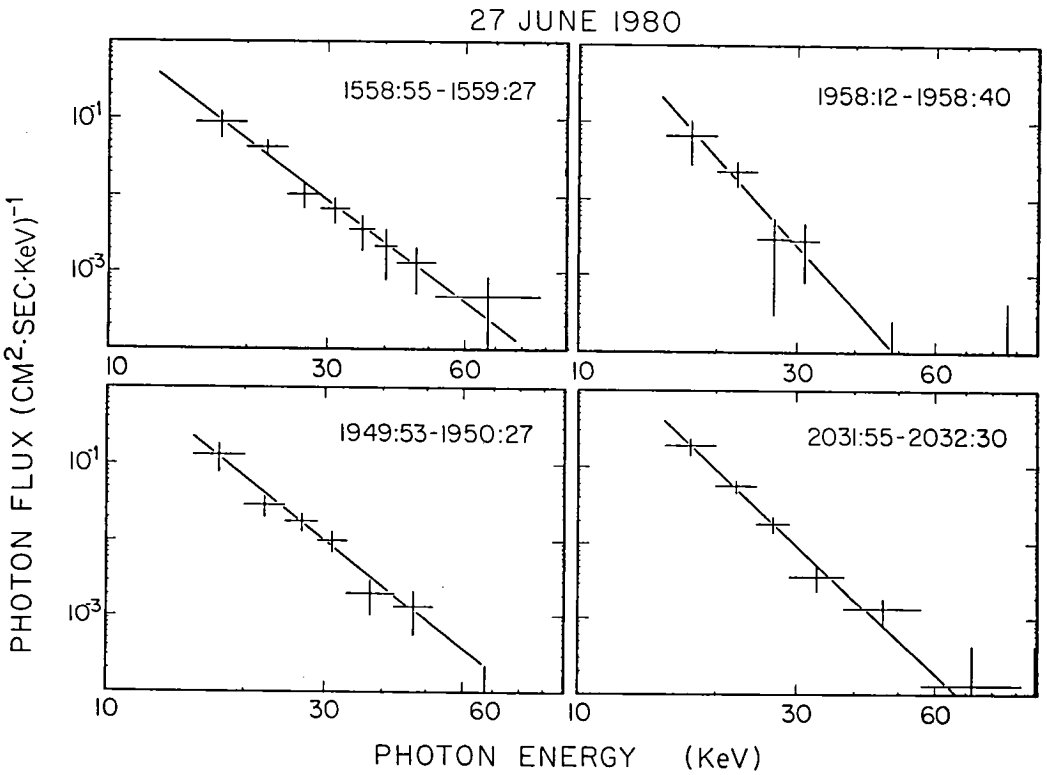

Figure 11. Photon energy spectra from the planar germanium detectors, integrated over each of the four bursts of Figure 10, are shown here (from Lin et al., 1984). The spectra are well-fitted by power laws $dJ/dE = AE^{-\gamma}$ with $\gamma \approx 4$ to 6.

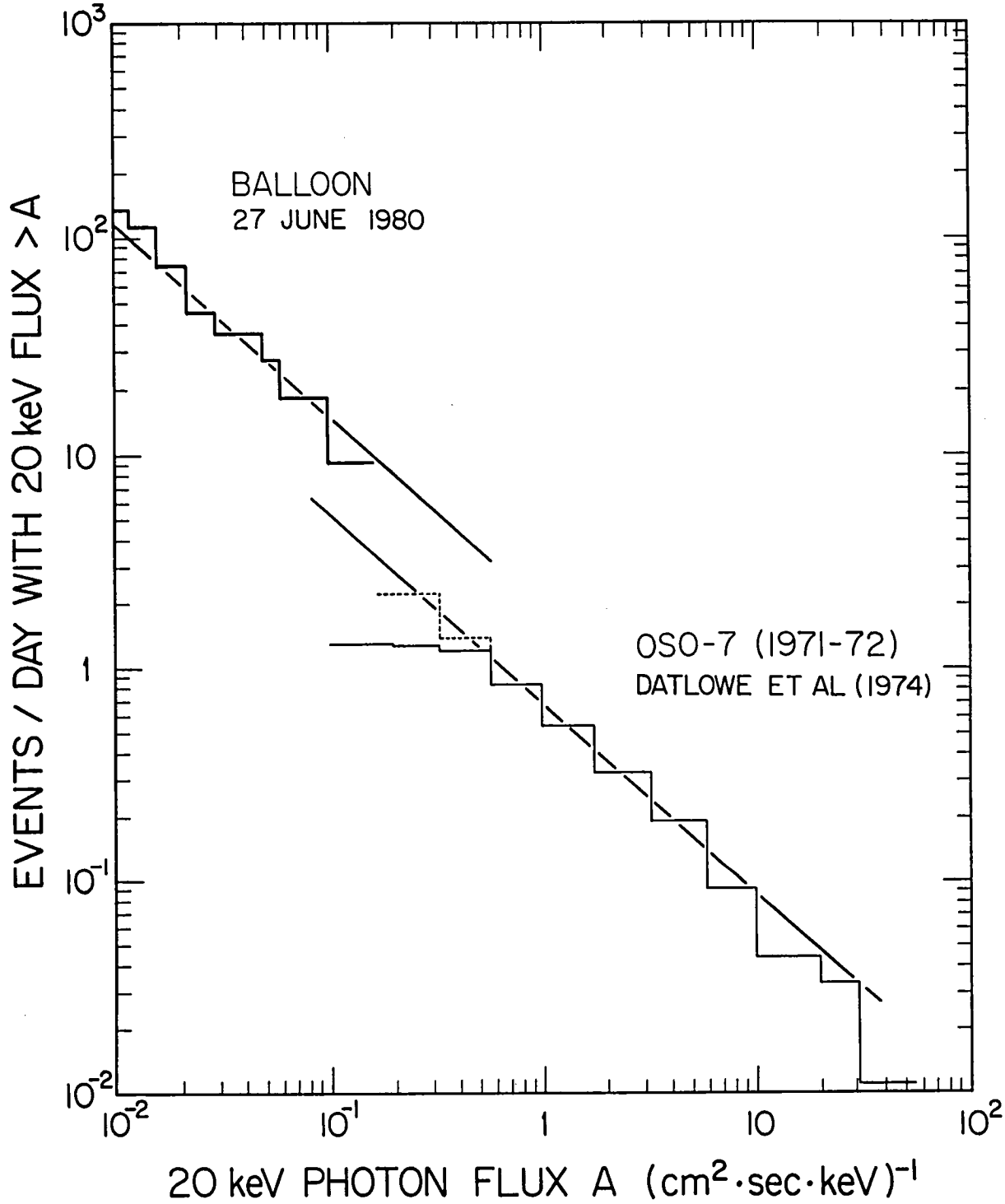

Figure 12. The distribution of the integral rate of occurrence of events versus peak 20 keV photon flux for the solar hard X-ray microflares observed in this balloon flight (from Lin et al., 1984). Also shown for comparison is the distribution of the solar flare hard X-ray bursts reported by Datlowe, Elcan, and Hudson (1974).

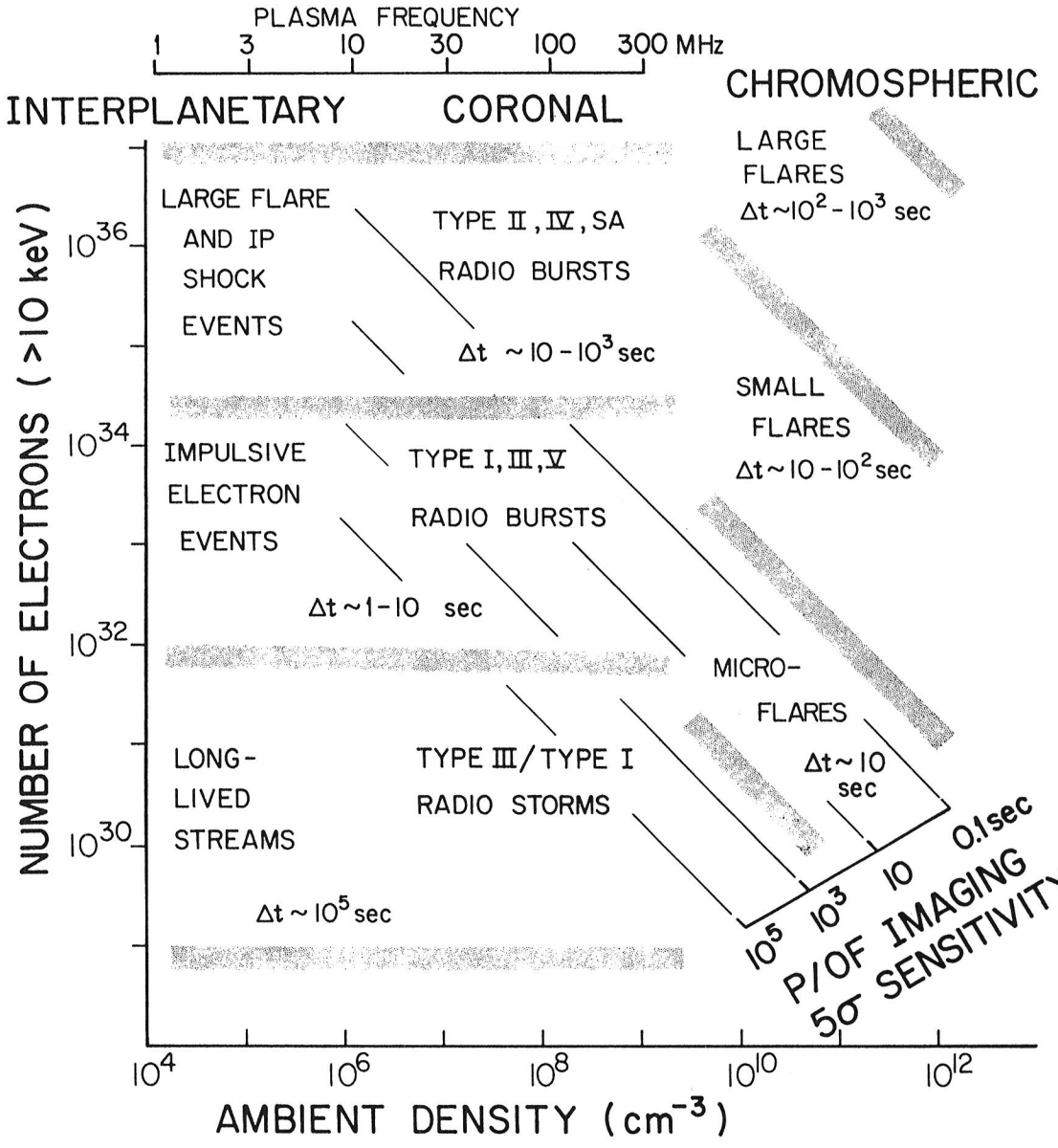

Figure 13. Various interplanetary, coronal, and chromospheric energetic electron phenomena are shown here. The number of >10 keV electrons involved (vertical scale) has been estimated from interplanetary observations at 1 AU except for the chromospheric phenomena which are given by hard X-ray observations. The estimated 5σ sensitivity for the planned P/OF hard X-ray instrumentation for different integration times is indicated by the diagonal lines.